MICRORESONATOR WITH GOLD NANOROD ARRAY FOR LASER WAVELENGTH MEASUREMENT BY PHOTO-THERMAL CONVERSION

Koji Sugano[1], Yuki Tanaka[1], Etsuo Maeda[2], Reo Kometani[2], and Yoshitada Isono[1]
[1]Department of Mechanical Engineering, Kobe University, Kobe, JAPAN
[2]Department of Mechanical Engineering, The University of Tokyo, Tokyo, JAPAN

ABSTRACT

In this study, we developed the resonator-based sensor device for measurement of laser wavelength changes in a wavelength division multiplexing (WDM) system for large capacity transmission. Laser light is absorbed into the gold nanorod array on the resonator beam, which has wavelength dependent absorption, resulting in temperature change of the beam. Therefore the wavelength change can be measured from resonant frequency shift. We observed the large resonant frequency shift when changing the laser wavelength. The shift was proportional to a cube of beam length and a laser power according to the developed equation. The maximum shift and resolution were 68.8 Hz/nm and 0.29 pm, respectively.

INTRODUCTION

A wavelength division multiplexing (WDM) has been used for large capacity transmission systems, which combines a number of optical signals with different wavelengths onto a single optical fiber. For larger capacity transmission, a channel spacing of laser wavelengths should be reduced. The various wavelength channels must be properly spaced to avoid interchannel interference.

A wavelength locker with a Fabry-perot etalon filter has conventionally been used for a 0.4- or 0.8-nm channel spacing system [1]. However the challenging issue has remains for a narrower channel spacing of 0.2 and 0.1 nm [2,3] because a wavelength measurement resolution of the conventional system is insufficient. The measurement resolution of 2.5 pm is required for the 0.1-nm channel spacing.

In this study, we developed the resonator-based sensor for measurement of laser wavelength changes with higher resolution than the conventional systems. The device consists of the doubly-clamped resonator beam and the gold nanorod array on the beam as an optical absorber of laser light. Effects of gold nanorod array and beam length on device performance were investigated in this experiment.

EXPERIMENTAL

Device Structure and Principle

Figure 1 shows a principle of laser wavelength measurement. As shown in Fig. 1(right), gold nanorods exhibit a characteristic absorption spectrum with peaks sue to plasmonic resonance depending on rod length, width and pitches [4-8] so that the wavelength change ($\Delta\lambda$) of the laser light causes the absorption change ($\Delta\beta$) on a gold nanorod array. The gold nanorod array was located on a resonator beam as an absorber as shown in Fig. 2(a). The beam temperature changes (ΔT) occurs by photo-thermal conversion when changing the absorption ($\Delta\beta$). The beam temperature changes is represented as the following equation.

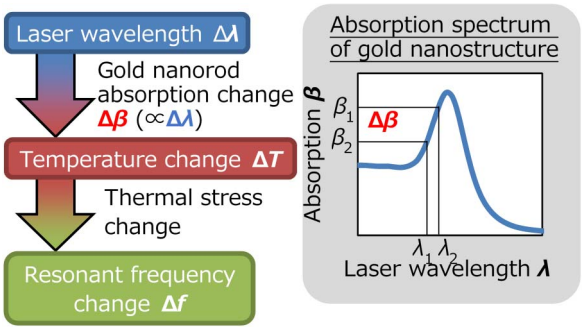

Figure 1: Principle of laser wavelength measurement.

$$\Delta T = \int_{-l/2}^{l/2} \frac{(l/2-|x|)\beta P}{\kappa w t}\frac{dx}{l} = \frac{l\beta P}{4wt\kappa} \qquad (1)$$

Here, l, w, t are length, width, and thickness of a beam, respectively as shown in Fig. 2(a). κ and P indicate thermal conductivity and laser power, respectively. The thermal stress change of the beam ($\Delta\sigma$) by the temperature change (ΔT) results in the resonant frequency shift (Δf) [9-13]. The resonant frequency f_σ under the thermal stress is represented as the following equation.

$$f_\sigma = f_0\sqrt{1+\frac{\sigma l^2}{3.4Et^2}} = f_0\sqrt{1-\frac{\alpha l^3\beta P}{13.6t^3w\kappa}}\ . \qquad (2)$$

Here E and α are Young's modulus and thermal expansion coefficient, respectively. The following equation is obtained as a simple form from Eq. (1).

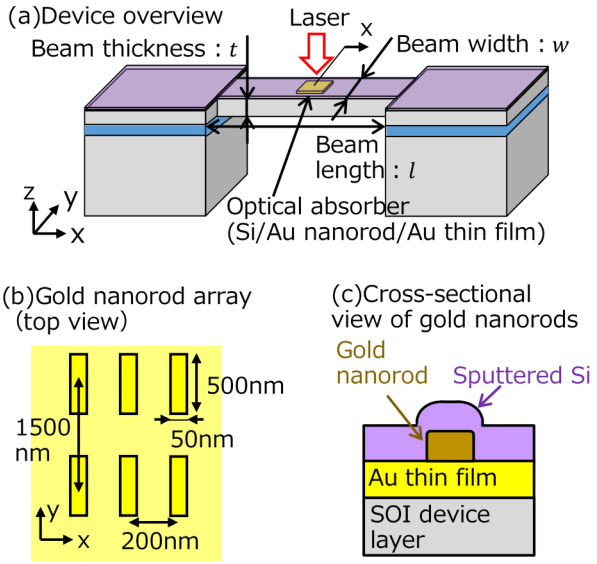

Figure 2: Schematics of the proposed device. (a)Overall view of the device, (b) width, length, pitches of gold nanorods (design), (c) cross-sectional view.

$$\frac{\Delta f}{f_0} = \frac{f_0 - f_\sigma}{f_0} = \frac{\alpha l^3 P}{27.2 t^3 w \kappa} \Delta\beta \,. \qquad (3)$$

This principle enables the measurement of the wavelength changes ($\Delta\lambda$) detecting the resonant frequency change (Δf). According to the Eq. (3), a resonant frequency change proportionally increased with absorption change ($\Delta\beta$), laser power (P), and the cube of beam length (l^3).

Figure 2 shows schematics of an overall device structure, nanorod array arrangement, and a cross-sectional structure. A doubly-clamped beam was fabricated from a SOI wafer. The absorber was located at the center of the beam. As shown in Fig. 2(b), gold nanorods with 50 nm width and 500 nm length were arranged with pitches of 200 and 1500 nm on 100-nm thick gold thin film, which was the optimized structure. Gold nanorods were covered by sputtered Si thin film as shown in Fig. 2(c) in order to adjust the peak wavelength in the absorption spectrum according to surrounding permittivity [5].

Device Fabrication

The device fabrication starts from a SOI wafer with a device layer thickness of 2 μm. After deposition of gold thin film, gold nanorods were fabricated by electron-beam lithography and lift-off process. Then backside and front side etchings were carried out for the resonator beam with width of 20 μm and length of 50~200 μm. Finally Si thin film was deposited on the resonator beam.

Measurement setup

An absorption spectra of the fabricated absorber structure were obtained using a microscopic spectrometer. From the measured reflection spectra, the absorption spectra were calculated.

Figure 3 shows the measurement setup for laser wavelength measurement. Resonant curves were measured using an optical heterodyne vibrometer with a He-Ne laser. A wavelength tunable laser with a 5-μm laser spot was used as an evaluation laser. A wavelength was varied from 1550 to 1564 nm with a 2-nm interval. The resonator was oscillated by the cyclic irradiation of a semiconductor laser of 488-nm wavelength. The device was placed in a vacuum chamber under the pressure of 10^{-3} Pa.

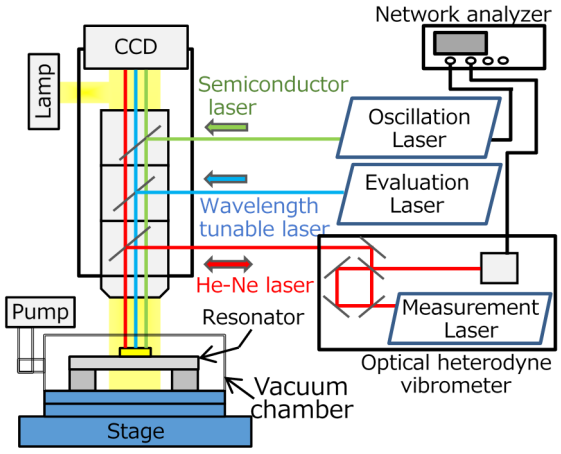

Figure 3: Schematic of laser wavelength measurement system.

RESULTS AND DISCUSSION

Fabrication

Figure 4 shows the SEM images of the fabricated device. The width and length of the fabricated nanorods shown in Fig. 4(b) were 67 and 501 nm on average. The measured thickness of the Si thin film was 61 nm.

Absorption Spectra

Figure 5 shows the measured absorption spectra of the fabricated absorber with and without the nanorod array.

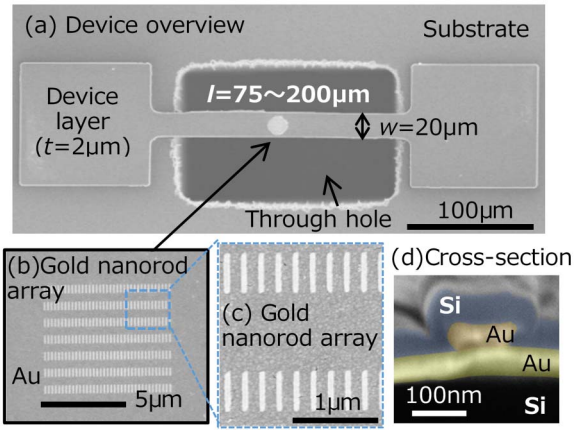

Figure 4: SEM images of the fabricated device (beam length : 200 μm) . (a) Overview of the structure, (b), (c) gold nanorod structuers, (d) cross-sectional view.

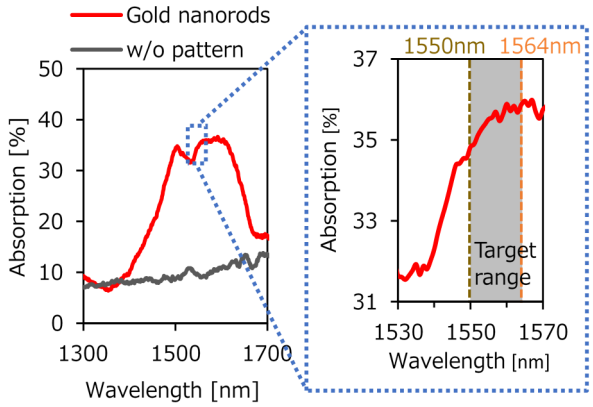

Figure 5: Optical absorption of the fabricated nanorod structures.

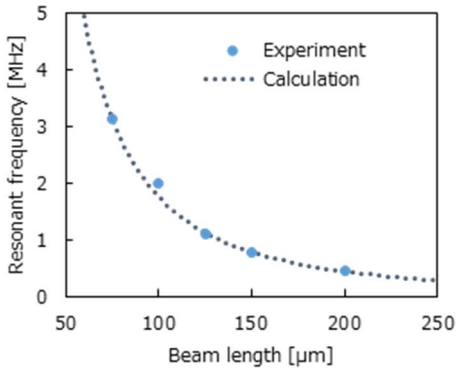

Figure 6: Measurement and calculation results of resonant frequency without laser irradiation as a function of beam length.

The nanorod array exhibits the slope of absorption at the target wavelength range although the structure without nanorods exhibits no absorption peaks.

Absorption Spectra

Figure 6 shows the measured and calculated resonant frequency without the evaluation laser irradiation. The experimental results show good agreement with the calculation.

Figures 7 and 8 show the measured resonance curves and the resonant frequency shift as a function of laser wavelength using the device with 200-μm length at the laser power of 1 mW. We observed the large resonant frequency shift with changing the laser wavelength from 1550 to 1564 nm although the structure without nanorod array showed no changes due to no absorption peaks in the target wavelength. The maximum change rate was 68.8 Hz/nm from 1552 to 1554 nm.

Figure 9 shows the resonant frequency shift as a function of laser wavelength depending on beam length. The resonant frequency shift increased with beam length as shown in Fig. 10. Figure 11 shows the resonant frequency shift as a function of a laser power in the case of 200-μm beam length. The resonant frequency decreased with increasing the laser power. According to these results, we confirmed the resonant frequency shift was proportional to a laser power and a cube of beam length. This tendency

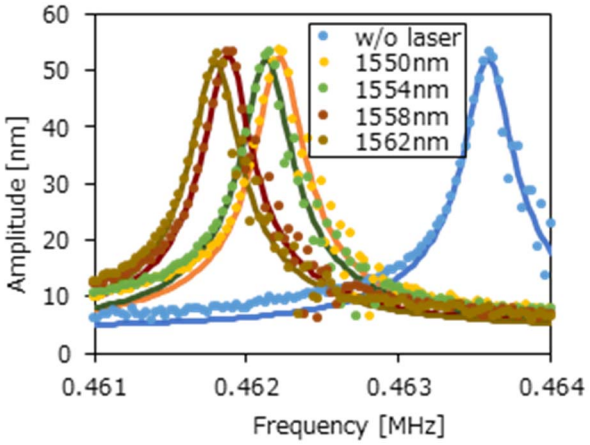

Figure 7: Resonant curves depending on laser wavelength at beam length of 200 μm.

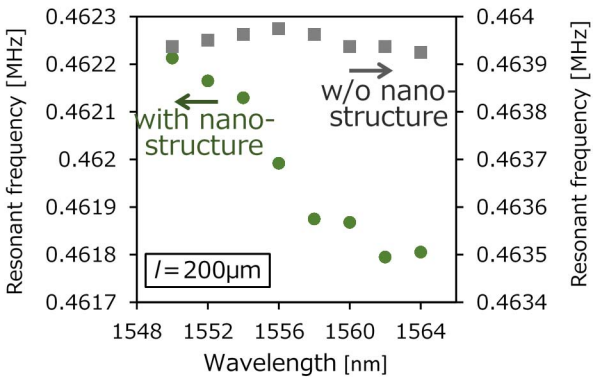

Figure 8: Resonant frequency changes with and without gold nanostructures at beam length of 200 μm.

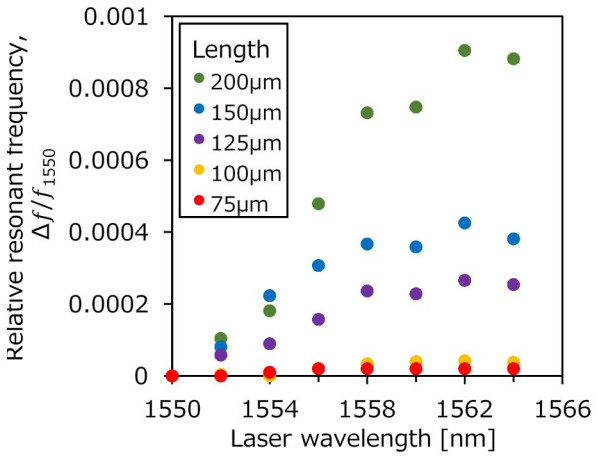

Figure 9: Resonant frequency changes depending on beam length and laser wavelength.

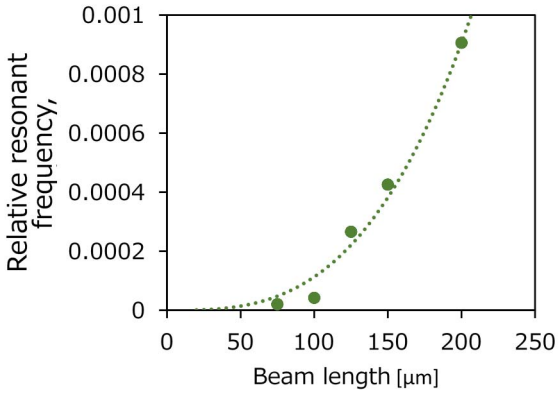

Figure 10: Relative resonant frequency change at 1560 nm as a function of beam length. The dotted line indicate the fitting result by the cube of beam length.

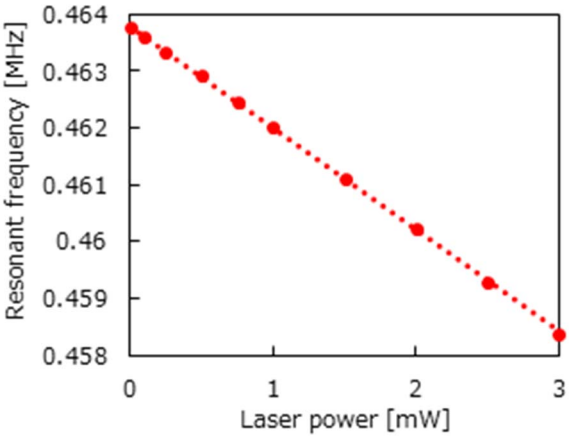

Figure 11: Resonant frequencies at 1560 nm as a function of evaluation laser power (beam length : 200 μm).

shows good agreement with the developed equation (Eq. 3).

The Q factor was calculated to be 2534 when the beam length and the laser power were 200 μm and 1 mW, respectively. The minimum resolution δf was calculated using the following equation considering thermal mechanical noise [14].

$$\delta f = \frac{1}{2\pi}\sqrt{\frac{k_B T f_0 \Delta f}{2\pi {f_0}^2 M_{eff}\langle {x_c}^2\rangle Q}} \,. \quad (4)$$

Here, k_B is Boltzmann's constant, T is the resonator temperature, M_{eff} is an effective mass, $\langle x_c \rangle$ is a mean square amplitude. The minimum resolution was calculated to be 0.29 pm. The developed device is expected for the wavelength measurement of the laser with high resolution.

CONCLUSION

The resonator-based sensor for measurement of laser wavelength changes with higher resolution than the conventional systems. The device consists of the doubly-clamped resonator beam and the gold nanorod array on the beam as an optical absorber of laser light for photo-thermal conversion. The nanorod array exhibits the slope of absorption at the target wavelength range. We observed the resonant frequency shift with changing the laser wavelength from 1550 to 1564 nm although the structure without the nanorod array showed no changes. The maximum change rate was 68.8 Hz/nm from 1552 to 1554 nm at the beam length of 200 μm. The resonant frequency shifts was proportional to a laser power and a cube of beam length according to the developed equation. The Q factor was calculated to be 2534. The minimum resolution was calculated to be 0.29 pm considering thermal mechanical noise. The developed device is expected for the wavelength measurement of the laser with high resolution.

ACKNOWLEDGEMENTS

A part of this study was supported by Micro/Nano Fabrication Hub in Kyoto University funded by the Ministry of Education, Culture, Sports, Science and Technology (MEXT), Japan.

REFERENCES

[1] Y. Yoon, J. Shim, D. Jang, J. Kim, Y. Eo, F. Rhee, "Transmission Spectra of Fabry–Perot Etalon Filter for Diverged Input Beams", *IEEE Photonics Technology Letters*, Vol. 14, No. 9, pp. 1315-1317, 2002.

[2] ITU-T, "Spectral grids for WDM applications: DWDM frequency grid series G: Transmission sysems and media, digital systems and networks", International Telecommunication Union, G.694.1, 2012.

[3] G. E. Keiser, "A Review of WDM Technology and Applications", *Optical Fiber Technology*, Vol. 5, pp. 3-39, 1999.

[4] K, Ueno, S. Juodkazis, M. Mino, V. Mizeikis, and H. Misawa, "Spectral Sensitivity of Uniform Arrays of Gold Nanorods to Dielectric Environment ", *The Journal of Phisical Chemistry C*, Vol. 111, No. 11, pp. 4180-4184, 2007.

[5] S. Link, M. B. Mohamed, and M. A. El-Sayed: "Simulation of the Optical Absorption Spectra of Gold Nanorods as a Function of Their Aspect Ratio and the Effect of the Medium Dielectric Constant", *Journal of Physical Chemistry B*, Vol. 103, pp. 3073-3077, 1999.

[6] O. L. Muskens, G. Bachelier, N. Del Fatti, F. Valle´e, A. Brioude, X. Jiang, M. P. Pileni, "Quantitative Absorption Spectroscopy of a Single Gold Nanorod", *Journal of Physical Chemistry C*, Vol. 112, pp. 8917-8921, 2008.

[7] Y. Ying, S.-S. Chang, C.-L. Lee, C. R. C. Wang, "Gold Nanorods: Electrochemical Synthesis and Optical Properties", *Journal of Physical Chemistry B*, Vol. 101, No. 34, pp. 6661-6664, 1997.

[8] P. K. Jain, K. S. Lee, I. H. El-Sayed, M. A. El-Sayed, "Calculated Absorption and Scattering Properties of Gold Nanoparticles of Different Size, Shape, and Composition: Applications in Biological Imaging and Biomedicine", *Journal of Physical Chemistry B*, Vol. 110, No. 14, pp. 7238-7248, 2006.

[9] H. Okamoto, T. Kamada, K. Onomitsu, I. Mahboob, H. Yamaguchi, "Optical Tuning of Coupled Micromechanical Resonators", *Applied Physics Express*, Vol. 2, No. 6, 062202, 2009.

[10] A. Bokaian, "Natural Frequencies of Beams Under Tensile Axial Loads", *Journal of Sound and Vibration*, Vol. 142, No. 3, pp. 481-498, 1990.

[11] S. C. Jun, X. M. H. Huang, M. Manolidis, C. A. Zorman, M. Mehregany, J. Hone, "Electrothermal tuning of Al–SiC nanomechanical resonators", *Nanotechnology*, Vol. 17, pp. 1506-1511, 2006.

[12] N. Inomata, T. Ono, "Thermal Sensor Probe with a Si Resonator in a Cavity for Thermal Insulation", *Japanese Journal of Applied Physics*, Vol. 52, 117201, 2013.

[13] N. Inomata, M. Toda, M. Sato, A. Ishijima, T. Ono, "Pico calorimeter for detection of heat produced in an individual brown fat cell", *Applied Physics Letters*, Vol. 100, 154104, 2012.

[14] K. L. Ekinci, Y. T. Yang, and M. L. Roukes: "Ultimate limits to inertial mass sensing based upon nanoelectromechanical systems", *Journal of Applied Physics*, Vol. 95, pp. 2682-2689, 2004.

CONTACT

*K. Sugano, tel: +81-78-803-6458;
sugano@mech.kobe-u.ac.jp